

Extension of Thin Wire Techniques in the FDTD Method for Debye Media

Dmitry Kuklin*

Abstract—There are applications of the finite difference time domain (FDTD) method, which need to model thin wires in dispersive media. However, existing thin wire techniques in the FDTD method are developed only for the conductive and dielectric media. The article presents a modification of oblique thin wire formalism proposed by Guiffaut et al. and a minor modification for the technique proposed by Railton et al. for applications with Debye media. The modifications are based on auxiliary differential equation (ADE) method. The modifications are validated by calculations of grounding potential rise (GPR) of a horizontal electrode buried in soil with dispersive properties.

1. INTRODUCTION

For particular simulations, there is a need to take into account frequency dependence of complex permittivity [1]. For example, a recent study [2] shows a significant influence of frequency dependent soil parameters on the grounding potential rise. As long as FDTD method has some strengths (such as modeling of inhomogeneities, for example), it is important to have an opportunity to use the method for calculations with thin wires in dispersive media. However, there is a number of difficulties in approximating the time domain expressions for the complex permittivity by finite differences [6]. On the other hand, there exist well-developed methods modeling Debye relaxation [18] which can be used as an approximation for the complex relative permittivity in a needed frequency range.

One can mark out two groups of techniques modeling thin wires in the FDTD method. In the first group, the FDTD equations for electric and magnetic field calculation are used to model the wire. Correct wire diameter is modeled by altering the FDTD equations [13, 14] or modifying parameters of the medium [15, 16]. The wire itself is modeled by using a high conductivity medium in the electric field calculation nodes locating along the wire (for the ideal conductor the electric field is set to zero in those nodes). In this work, the technique proposed by Railton et al. [16] and improved by Taniguchi et al. [17] is used. In the second group, two additional equations are used to model the current and voltage waves propagating along the wire. The technique was originally proposed by Holland and Simpson [8] and improved by number of authors [10–12]. The oblique thin wire formalism [12] is seemingly the only method to this moment allowing to model arbitrarily oriented thin wires (which radius is not specified by the cell size) in the FDTD method with rectangular mesh. However, in order to use these techniques in Debye media, they need to be modified.

Received 18 August 2016, Accepted 29 September 2016, Scheduled 13 October 2016

* Corresponding author: Dmitry Kuklin (kuklindima@gmail.com).

The author is with the Centre for Physical and Technological Problems of Energy in Northern Areas of Kola Science Centre of the Russian Academy of Sciences, Apatity, Russian Federation.

2. OVERVIEW OF AUXILIARY DIFFERENTIAL EQUATION METHOD FOR DEBYE MEDIA

One of the approaches to model dispersive materials in the FDTD method is the auxiliary differential equation method [7, 18]. This is an efficient algorithm that adds a relatively small amount of floating-point operations and storage needed for unknowns to basic FDTD algorithm. It is convenient to make an overview of ADE method.

Ampere's law for Debye medium in the frequency domain is

$$\nabla \times \hat{\mathbf{H}} = \epsilon_0 \epsilon_\infty j\omega \hat{\mathbf{E}} + \sigma \hat{\mathbf{E}} + \sum_{p=1}^P \hat{\mathbf{J}}_p, \quad (1)$$

where $\hat{\mathbf{H}}$ is the magnetic field, $\hat{\mathbf{E}}$ the electric field, ϵ_0 the vacuum permittivity, ϵ_∞ the permittivity at the high frequency limit, σ the conductivity, P the number of Debye poles, and $\hat{\mathbf{J}}_p$ the polarization current for the p 'th Debye pole:

$$\hat{\mathbf{J}}_p = \frac{\epsilon_0 \Delta \epsilon_p j\omega}{1 + j\omega \tau_p} \hat{\mathbf{E}}, \quad (2)$$

where τ_p is the relaxation time, $\Delta \epsilon_p = \epsilon_p - \epsilon_\infty$ (where ϵ_p is the low frequency permittivity). Multiplication of both sides of Equation (2) by $(1 + j\omega \tau_p)$ and applying inverse Fourier transform gives

$$\mathbf{J}_p + \tau_p \frac{\partial \mathbf{J}_p}{\partial t} = \epsilon_0 \Delta \epsilon_p \frac{\partial \mathbf{E}}{\partial t}. \quad (3)$$

In the finite difference form, using $\mathbf{J}_p^{n+1/2} = (\mathbf{J}_p^n + \mathbf{J}_p^{n+1})/2$ (time moment is determined as $t = n\Delta t$), Equation (3) can be approximated as

$$\frac{\mathbf{J}_p^n + \mathbf{J}_p^{n+1}}{2} + \tau_p \frac{\mathbf{J}_p^{n+1} - \mathbf{J}_p^n}{\Delta t} = \epsilon_0 \Delta \epsilon_p \frac{\mathbf{E}^{n+1} - \mathbf{E}^n}{\Delta t}. \quad (4)$$

Solving this for \mathbf{J}_p^{n+1} gives

$$\mathbf{J}_p^{n+1} = k_p \mathbf{J}_p^n + \beta_p \frac{\mathbf{E}^{n+1} - \mathbf{E}^n}{\Delta t}, \quad (5)$$

where

$$k_p = \frac{1 - \Delta t/(2\tau_p)}{1 + \Delta t/(2\tau_p)}, \quad \beta_p = \frac{\epsilon_0 \Delta \epsilon_p \Delta t / \tau_p}{1 + \Delta t/(2\tau_p)}. \quad (6)$$

So that updating of polarization current \mathbf{J}_p is performed by Equation (5).

Next, an electric field updating equation should be obtained. Using the Equation (5), $\mathbf{J}_p^{n+1/2}$ can be evaluated from \mathbf{E}^n , \mathbf{E}^{n+1} and \mathbf{J}^n :

$$\mathbf{J}_p^{n+1/2} = \frac{\mathbf{J}_p^n + \mathbf{J}_p^{n+1}}{2} = \frac{1}{2} \left[(1 + k_p) \mathbf{J}_p^n + \beta_p \frac{\mathbf{E}^{n+1} - \mathbf{E}^n}{\Delta t} \right], \quad (7)$$

then it can be substituted into the time domain form of Equation (1) approximated by the finite differences:

$$\nabla \times \mathbf{H}^{n+1/2} = \epsilon_0 \epsilon_\infty \frac{\mathbf{E}^{n+1} - \mathbf{E}^n}{\Delta t} + \sigma \frac{\mathbf{E}^{n+1} + \mathbf{E}^n}{2} + \frac{1}{2} \sum_{p=1}^P \left[(1 + k_p) \mathbf{J}_p^n + \beta_p \frac{\mathbf{E}^{n+1} - \mathbf{E}^n}{\Delta t} \right], \quad (8)$$

and the electric field at $n + 1$ can be calculated:

$$\mathbf{E}^{n+1} = \frac{2\epsilon_0 \epsilon_\infty + \sum_{p=1}^P \beta_p - \sigma \Delta t}{2\epsilon_0 \epsilon_\infty + \sum_{p=1}^P \beta_p + \sigma \Delta t} \mathbf{E}^n + \frac{2\Delta t}{2\epsilon_0 \epsilon_\infty + \sum_{p=1}^P \beta_p + \sigma \Delta t} \cdot \left[\nabla \times \mathbf{H}^{n+1/2} - \frac{1}{2} \sum_{p=1}^P (1 + k_p) \mathbf{J}_p^n \right]. \quad (9)$$

With this method first the electric field is calculated using Equation (9). Then the polarization current is calculated with Equation (5). Finally, the magnetic field is obtained from the usual FDTD expression.

3. MODIFICATION OF THE MODEL PROPOSED BY GUIFFAUT ET AL.

Each method, based on the approach of Holland and Simpson, uses two equations to model propagation of waves along the wire:

$$L \frac{\partial I}{\partial t} + \frac{\partial V}{\partial z} + RI = E_z(d), \quad (10)$$

$$C_l \frac{\partial V}{\partial t} + \frac{\partial I}{\partial z} + \frac{\sigma C_l V}{\epsilon_0 \epsilon_\infty} = 0, \quad (11)$$

where I is the current; V is the voltage; C_l , L and R are respectively the capacitance, the inductance and the resistance per unit length; E_z is the electric field longitudinal to the wire at the distance d from the wire. Applying ADE approach, the second equation is modified and one more equation is added.

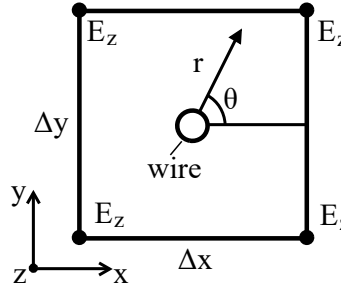


Figure 1. Thin wire and closest electric field nodes of the FDTD grid.

Figure 1 shows a thin wire oriented along z -axis and closest electric field nodes. The θ component of the Faraday's law in cylindrical coordinates:

$$\frac{\partial E_r}{\partial z} - \frac{\partial E_z}{\partial r} = -\mu \frac{\partial H_\theta}{\partial t}. \quad (12)$$

Equation (10) is derived by taking the integral of Equation (12) from $r = a$ (where a is wire radius) to d

$$\int_a^d \frac{\partial E_r}{\partial z} - \int_a^d \frac{\partial E_z}{\partial r} = -\mu \int_a^d \frac{\partial H_\theta}{\partial t} \quad (13)$$

and substituting approximations for the magnetic and electric field around the wire (here Q is the charge per unit length) [8]:

$$H_\theta = \frac{I}{2\pi r}, \quad E_r = \frac{Q}{2\pi r \epsilon_0 \epsilon_\infty} = \frac{C_l V}{2\pi r \epsilon_0 \epsilon_\infty}. \quad (14)$$

The RI takes into account the resistance of the wire [12]. The L is defined by

$$L = \frac{\mu_0}{2\pi} \ln(d/a). \quad (15)$$

Equation (11) is derived from the Ampere's law in a similar manner as the modified version below (with the exception that the modified version takes into account the polarization current).

The modification starts from the radial component of Ampere's law equation in cylindrical coordinates:

$$\frac{1}{r} \frac{\partial H_z}{\partial \theta} - \frac{\partial H_\theta}{\partial z} = j\omega \epsilon_0 \epsilon_\infty E_r + \sigma E_r + \sum_{p=1}^P J_{r_p}. \quad (16)$$

Integration of the equation from $\theta = 0$ to 2π yields

$$\frac{1}{r} \frac{\partial}{\partial \theta} \int_0^{2\pi} H_z d\theta - \frac{\partial}{\partial z} \int_0^{2\pi} H_\theta d\theta = j\omega \epsilon_0 \epsilon_\infty \int_0^{2\pi} E_r d\theta + \sigma \int_0^{2\pi} E_r d\theta + \sum_{p=1}^P \int_0^{2\pi} J_{r_p} d\theta. \quad (17)$$

Using Equation (14) and approximating the derivative $\partial I/\partial z$ by finite difference, Equation (17) becomes

$$I_{k+1/2} - I_{k-1/2} + j\omega CV + \frac{\sigma CV}{\epsilon_0 \epsilon_\infty} + \sum_{p=1}^P J'_{r_p} = 0, \quad (18)$$

where C is equivalent capacitance for particular node k (in [12], C_k is used), and J'_{r_p} equals

$$J'_{r_p} = \frac{\Delta \epsilon_p j \omega}{\epsilon_\infty (1 + j \omega \tau_p)} CV. \quad (19)$$

In a similar manner as earlier, an update equation for the J'_{r_p} can be obtained:

$$J'^{n+1}_{r_p} = k'_p J'^n_{r_p} + \beta'_p C \frac{V^{n+1} - V^n}{\Delta t}, \quad (20)$$

where

$$k'_p = \frac{1 - \Delta t/(2\tau_p)}{1 + \Delta t/(2\tau_p)}, \quad \beta'_p = \frac{\Delta \epsilon_p \Delta t/\tau_p}{\epsilon_\infty + \epsilon_\infty \Delta t/(2\tau_p)}. \quad (21)$$

Approximation of time domain version of Equation (18) by finite differences with using $J'^{n+1/2}_{r_p} = (J'^n_{r_p} + J'^{n+1}_{r_p})/2$ leads to

$$-\left(I_{k+1/2}^{n+1/2} - I_{k-1/2}^{n+1/2}\right) = C \frac{V^{n+1} - V^n}{\Delta t} + \sigma C \frac{V^{n+1} + V^n}{2\epsilon_0 \epsilon_\infty} + \frac{1}{2} \sum_{p=1}^P \left[(1 + k'_p) J'^n_{r_p} + \beta'_p C \frac{V^{n+1} - V^n}{\Delta t} \right]. \quad (22)$$

Now the voltage at $n + 1$ can be calculated:

$$V^{n+1} = b_1 V^n - \frac{b_2}{C} \cdot \left[I_{k+1/2}^{n+1/2} - I_{k-1/2}^{n+1/2} + \frac{1}{2} \sum_{p=1}^P (1 + k'_p) J'^n_{r_p} \right], \quad (23)$$

where

$$b_1 = \frac{2\epsilon_0 \epsilon_\infty + \epsilon_0 \epsilon_\infty \sum_{p=1}^P \beta'_p - \sigma \Delta t}{2\epsilon_0 \epsilon_\infty + \epsilon_0 \epsilon_\infty \sum_{p=1}^P \beta'_p + \sigma \Delta t}, \quad b_2 = \frac{2\epsilon_0 \epsilon_\infty \Delta t}{\left(2\epsilon_0 \epsilon_\infty + \epsilon_0 \epsilon_\infty \sum_{p=1}^P \beta'_p + \sigma \Delta t \right)}. \quad (24)$$

Accordingly, calculation of the voltage in a multiwire junction [12] should be modified also:

$$V^{n+1} = b_1 V^n + \frac{b_2}{C_{eq,0}} \cdot \left[\sum_{q=1}^{N_w} I_q^{n+1/2} - \frac{1}{2} \sum_{p=1}^P (1 + k'_p) J''^n_{r_p} \right], \quad (25)$$

where N_w is the number of wires in the junction [12] and $C_{eq,0}$ the equivalent capacitance for the junction [12]. The update equation for the J''_{r_p} is

$$J''^{n+1}_{r_p} = k'_p J''^n_{r_p} + \beta'_p C_{eq,0} \frac{V^{n+1} - V^n}{\Delta t}. \quad (26)$$

The current from the wire is distributed by the FDTD grid by means of the current sources. Therefore, the electric field at time step n in Equation (9) should be saved before the wire current is distributed. The saved electric field is used then in a calculation of the polarization current by the Equation (5).

Summing up, the modification implies using Equations (23) and (25) instead of those presented in the [12] and calculation of the J'_{r_p} and J''_{r_p} by Equations (20) and (26). Other peculiarities of the method (such as calculation of the inductance per unit length, distribution of the wire current by the FDTD grid etc.) remain unchanged.

4. MODIFICATION OF THE MODEL PROPOSED BY RAILTON ET AL.

The technique proposed by Railton et al. [16] is based on the correction of electric and magnetic fields in the nodes adjacent to the wire. Modeling of the wire itself is performed either by setting the electric field to zero along the electric field nodes or using a highly conductive medium.

According to the technique [16], the permittivity and the permeability in the nodes adjacent to z -directed wire should be multiplied by the coefficients ϵ_x , ϵ_y , μ_x , μ_y :

$$\mu_x = \frac{1}{\epsilon_y} = \frac{\ln\left(\frac{\Delta y}{a}\right)}{2 \arctan\left(\frac{\Delta x}{\Delta y}\right)} \frac{\Delta x}{\Delta y}, \quad \mu_y = \frac{1}{\epsilon_x} = \frac{\ln\left(\frac{\Delta x}{a}\right)}{2 \arctan\left(\frac{\Delta y}{\Delta x}\right)} \frac{\Delta y}{\Delta x}, \quad (27)$$

where a is the wire radius, and Δx and Δy are respectively x and y dimensions of the cell. If the wire is located in the conductive medium the conductivity should also be altered [17], and $\sigma_x = \epsilon_x$, $\sigma_y = \epsilon_y$.

To use this technique in Debye media, $\Delta\epsilon$ should be corrected as well by $\Delta\epsilon_x = \epsilon_x$ and $\Delta\epsilon_y = \epsilon_y$. This can be achieved by altering β_p in Equation (6). As long as in the model of Noda and Yokoyama [15] the permittivity is corrected in a similar way, the same correction of $\Delta\epsilon$ should be applicable to the model [15] too.

5. VALIDATION

In order to validate the proposed modifications, the calculations of the GPR for a buried horizontal electrode have been carried out by the FDTD method. Then the calculation results have been compared to those simulated using the hybrid electromagnetic model (HEM) which is validated experimentally [5].

First, the complex permittivity should be approximated with the Debye relaxation function. From the empirical expression in the work of [5] the imaginary part of the permittivity can be evaluated:

$$\epsilon_r''(f) = \frac{1.2 \cdot 10^{-6} \sigma_0^{0.27} \cdot (f - 100)^{0.65}}{2\pi f \epsilon_0}, \quad (28)$$

where f is the frequency in Hz and σ_0 a soil conductivity ($\sigma_0 = 1/\rho_0$). The frequency range for f in formula (28) is 100 Hz–4 MHz [5]. The real part of the permittivity [5]:

$$\epsilon_r'(f) = 7.6 \cdot 10^3 f^{-0.4} + 1.3. \quad (29)$$

The frequency range for Equation (29) is 10 kHz–4 MHz. For the range 100 Hz–10 kHz, it is suggested in [5] to use constant permittivity equaled to the permittivity at frequency 10 kHz. However, for the calculations in the present work, the frequency range 10 kHz–4 MHz is enough.

The n -term Debye function expansion is defined by

$$\hat{\epsilon}_r(\omega) = \epsilon_\infty + \sum_{p=1}^n \frac{\Delta\epsilon_p}{1 + j\omega\tau_p}. \quad (30)$$

To calculate the parameters ϵ_∞ , $\Delta\epsilon$, and τ , a hybrid particle swarm-least squares optimization approach was used [6]. The obtained four-term expansion parameters for the soils with resistivity $2000 \Omega \cdot \text{m}$ and $4000 \Omega \cdot \text{m}$ are listed in Table 1. Fig. 2 shows the real and imaginary parts of the Debye function expansion compared to those of the empirical functions for 10 kHz–4 MHz frequency range.

It should be noted that the real and imaginary parts of the permittivity are related to each other by the Kramers-Kronig relations [6, 19]. However, Equations (28) and (29) do not obey these relations because the imaginary part depends on the ρ_0 while the real part does not (in other words, the imaginary part of the permittivity is not related to the real part mathematically). For this reason, it is not possible to approximate both equations exactly for all soils by the Debye function expansion (but a good approximation is possible for soils with ρ_0 close to about $2000 \Omega \cdot \text{m}$). Therefore, here the imaginary part was approximated more exactly than the real part.

In order to perform lengthy calculations (thousands of time steps) in a reasonable amount of time, the volume size should be relatively small, which, in the case of GPR simulations, can be achieved

Table 1. The ϵ_∞ , $\Delta\epsilon$, and τ parameters of the four-term expansion used to approximate empirical expressions.

$\rho_0, \Omega \cdot \text{m}$	ϵ_∞	$\Delta\epsilon_1$	τ_1, s	$\Delta\epsilon_2$	τ_2, s	$\Delta\epsilon_3$	τ_3, s	$\Delta\epsilon_4$	τ_4, s
2000	13.120	210.820	$2.498 \cdot 10^{-5}$	59.823	$3.484 \cdot 10^{-6}$	35.472	$6.032 \cdot 10^{-7}$	22.768	$7.462 \cdot 10^{-8}$
4000	23.282	173.829	$2.374 \cdot 10^{-5}$	49.872	$3.103 \cdot 10^{-6}$	27.992	$5.056 \cdot 10^{-7}$	17.445	$6.452 \cdot 10^{-8}$

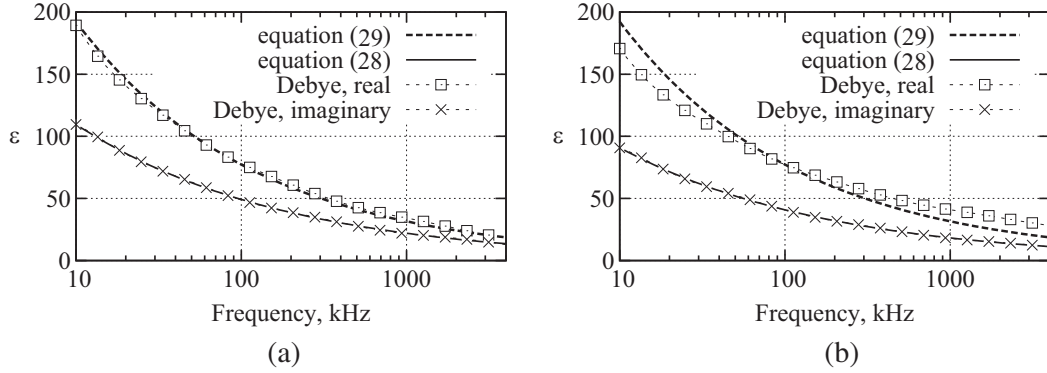


Figure 2. Approximation of the permittivity with Debye relaxation. (a) $2000 \Omega \cdot \text{m}$, (b) $4000 \Omega \cdot \text{m}$.

by modeling the current lead wire and the voltage reference wire as infinite. In the FDTD method, wires are simulated infinite when they penetrate absorbing boundary condition (ABC). The uniaxial perfectly matched layer (UPML) is used as the ABC in the article. In the methods based on the thin wire formalism of Holland and Simpson [8], the wire current is distributed in the FDTD calculation grid by means of the current sources. However, the UPML is not intended to contain current sources. Therefore, when the wire penetrates UPML region this can lead to a calculation error. On the contrary, the wire simulated by modifying the medium parameters can penetrate UPML region without causing the error. As long as a wire modeled by the formalism of Holland and Simpson (or model of Guiffaut et al.) can be located in a conductive medium, it is possible to place this wire in the same location as a wire simulated by model of Railton et al. (because this wire is modeled simply by using a conductive medium along the nodes of the electric field grid).

This way of modeling infinite wires can be verified by calculations with two volumes having different sizes (see Fig. 3). The size of the cell for the computation mesh is 0.125 m (the mesh has the cubic form). The thickness of the UPML equals 15 cells. The current lead wire, voltage reference wire, and grounding electrode are located perpendicularly to each other in order to minimize magnetic influence between the wires. The diameter of all the wires is 14 mm .

To calculate the potential difference between two wires (the grounding rod and the voltage reference wire), their ends (or nodes) are located at the same point without electrical connection between the wires. Voltage difference equals to a difference between potentials of the wire nodes. There is an alternative way to calculate the voltage difference [3].

The form of the current of the ideal current source is set by function

$$i(t) = \begin{cases} 0.5 + 0.5 \sin(t\pi/t_1 - 0.5\pi) & \text{if } t \leq t_1 \\ 1 & \end{cases} \quad (31)$$

where $t_1 = 0.1 \cdot 10^{-6} \mu\text{s}$. The current amplitude is 1 A .

The GPR simulation results for the two different volumes are shown in Fig. 4 (the calculations are carried for the soil with dispersion). It can be seen that they agree with each other exactly.

The validation calculation model is shown in Fig. 5. The computation mesh and ABC parameters are the same as earlier. For the wires modeled by the Railton's technique, the voltage between the

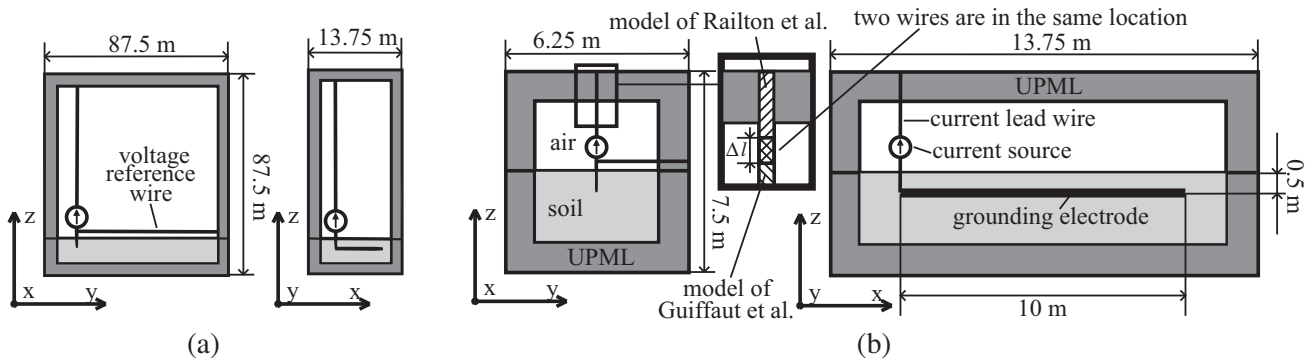


Figure 3. Calculation models to verify infinite wires modeling. (a) Bigger volume for the reference simulations, (b) smaller volume with modeling of infinite wires. Δl is the cell size.

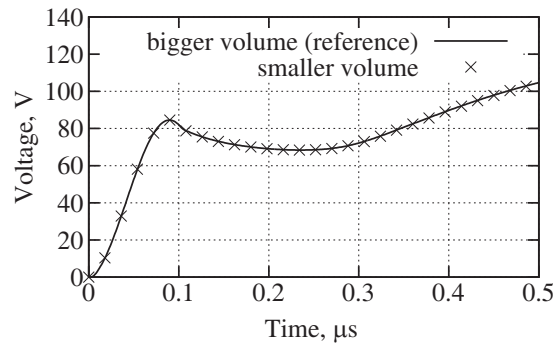


Figure 4. GPR calculation results for two different volumes. $\rho_0 = 2000 \Omega \cdot m$.

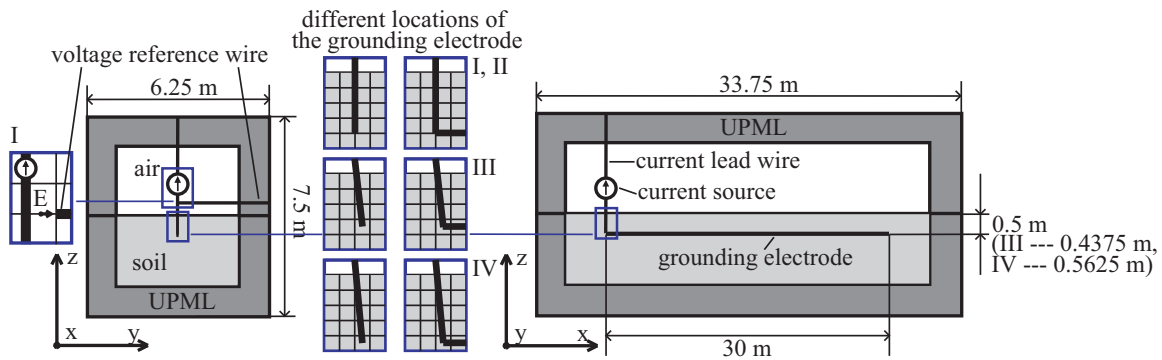


Figure 5. Calculation model for validation of the modifications. I — model of Railton et al.; II, III, IV — model of Guiffaut et al.

grounding electrode and the voltage reference wire is calculated as the electric field in the node between the wires times the cell size: $V = E\Delta l$, where Δl is the FDTD cell size. In the case of the model of Guiffaut et al., the grounding electrode was located differently: along the nodes of the FDTD grid and with a shift. The start and the end of the shifted grounding electrode were placed in the centers of the electric field grid cells. Using 0.125 m cell size this means that the grounding electrode cannot be placed at the depth 0.5 m exactly. To ensure that the depth does not influence significantly, the calculations were carried for the grounding electrode located $0.5\Delta l$ higher and $0.5\Delta l$ lower than 0.5 m depth.

The current form is set by [4]

$$i(t) = \sum_{k=1}^m \frac{I_{0k}}{\eta_k} \exp\left(-\frac{t}{\tau_{2k}}\right) \frac{(t/\tau_{1k})^{n_k}}{1 + (t/\tau_{1k})^{n_k}}, \quad \eta_k = \exp\left(-\frac{\tau_{1k}}{\tau_{2k}}\right) \left(\frac{n_k \tau_{2k}}{\tau_{1k}}\right)^{1/n_k}, \quad (32)$$

where $I_{01} = 15.4$ kA, $I_{02} = 7.2$ kA, $n_1 = 3.4$, $n_2 = 2$, $\tau_{11} = 0.6$ μ s, $\tau_{12} = 4$ μ s, $\tau_{21} = 4$ μ s, $\tau_{22} = 120$ μ s.

The calculation results are shown in Fig. 6 (the simulations are carried not only for the dispersive soil but also for the soil with constant permittivity). It is seen from the figure that FDTD method simulation results are in good agreement with those of the HEM method. The difference between the results of these two methods is approximately the same both for the cases with dispersion and without it, which indicates that the difference is caused by peculiarities of the methods (or models) itself related to the injection of the current into the grounding electrode and calculation of the voltage rather than inaccuracies of the proposed modifications.

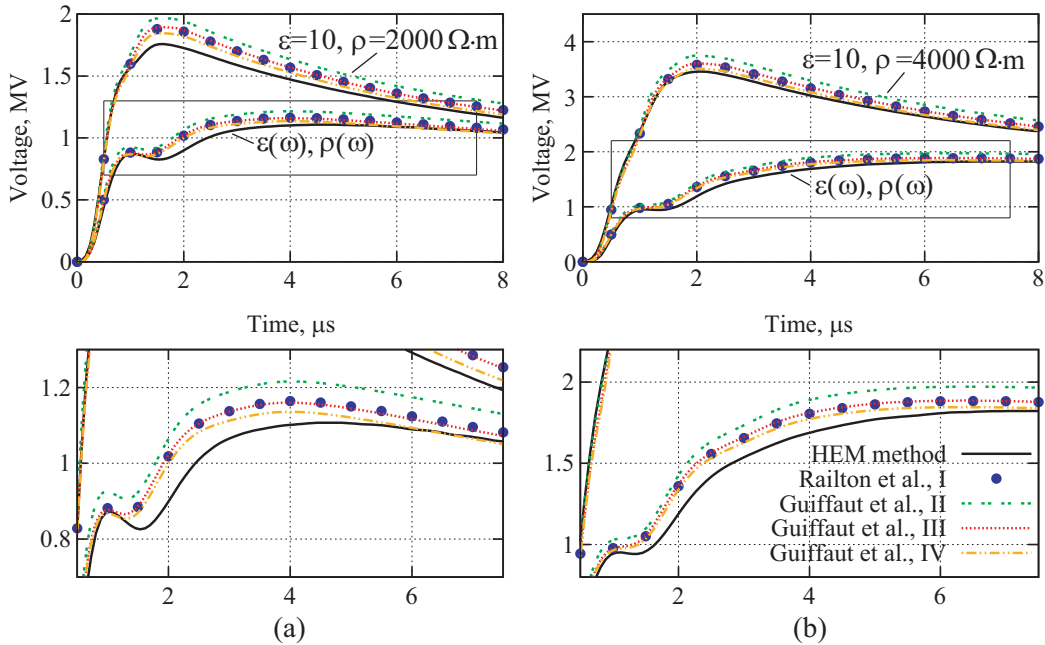


Figure 6. GPR of the horizontal electrode simulated by different methods. HEM method simulation results are adopted from [2]. (a) $\rho_0 = 2000 \Omega \cdot \text{m}$, (b) $\rho_0 = 4000 \Omega \cdot \text{m}$.

6. CONCLUSIONS

The modifications of the thin wire model proposed by Guiffaut et al. and the model proposed by Railton et al. are presented. With the proposed modifications, it is now possible to perform calculations with thin wires located in Debye media in the FDTD method, which is important, for example, for simulations involving wires located in soils with dispersive properties. As long as the modifications are based on the efficient ADE method, their implementation adds a relatively small amount of floating-point operations and storage needed for unknowns to the thin wire models (in the case of the model proposed by Railton et al., only a correction of the coefficients is needed). It is expected that thin wires in other media (such as Lorenz and Drude) can be modeled similarly with the ADE method.

REFERENCES

1. Kuklin, D., "Choosing configurations of transmission line tower grounding by back flashover probability value," *Front. Energy*, Vol. 10, No. 2, 213–226, 2016.

2. Alipio, R. and S. Visacro, "Frequency dependence of soil parameters: effect on the lightning response of grounding electrodes," *IEEE Trans. Electromagn. Compat.*, Vol. 55, No. 1, 132–139, 2013.
3. Diaz, L., C. Miry, A. Reineix, C. Guiffaut, and A. Tatematsu, "FDTD transient analysis of grounding grids. A comparison of two different thin wire models," *2015 IEEE International Symposium on Electromagnetic Compatibility (EMC)*, 501–506, 2015.
4. De Conti, A. and S. Visacro, "Analytical representation of single- and double-peaked lightning current waveforms," *IEEE Trans. Electromagn. Compat.*, Vol. 49, No. 2, 448–451, 2007.
5. Visacro, S. and R. Alipio, "Frequency dependence of soil parameters: experimental results, predicting formula and influence on the lightning response of grounding electrodes," *IEEE Trans. Power Delivery*, Vol. 27, No. 2, 927–935, 2012.
6. Kelley D. F., T. J. Destan, and R. J. Luebbers, "Debye function expansions of complex permittivity using a hybrid particle swarm-least squares optimization approach," *IEEE Trans. Antennas Propag.*, Vol. 55, No. 7, 1999–2005, 2007.
7. Okoniewski, M., M. Mrozowski, and M. A. Stuchly, "Simple treatment of multi-term dispersion in FDTD," *IEEE Microw. Guided Wave Lett.*, Vol. 7, No. 5, 121–123, 1997.
8. Holland, R. and L. Simpson, "Finite-difference analysis of EMP coupling to thin struts and wires," *IEEE Trans. Electromagn. Compat.*, Vol. 23, No. 2, 88–97, 1981.
9. Guiffaut, C. and A. Reineix, "Cartesian shift thin wire formalism in the FDTD method with multiwire junctions," *IEEE Trans. Antennas Propag.*, Vol. 58, No. 8, 2658–2665, 2010.
10. Ledfelt, G., "A stable subcell model for arbitrarily oriented thin wires for the FDTD method," *Int. J. Numer. Model. Electron. Netw. Devices Fields*, Vol. 15, No. 5–6, 503–515, 2002.
11. Edelvik, F., "A new technique for accurate and stable modeling of arbitrarily oriented thin wires in the FDTD method," *IEEE Trans. Electromagn. Compat.*, Vol. 45, No. 2, 416–423, 2003.
12. Guiffaut, C., A. Reineix, and B. Pecqueux, "New oblique thin wire formalism in the FDTD method with multiwire junctions," *IEEE Trans. Antennas Propag.*, Vol. 60, No. 3, 1458–1466, 2012.
13. Umashankar, K. and A. Taflove, "Calculation and experimental validation of induced currents on coupled wires in an arbitrary shaped cavity," *IEEE Trans. Antennas Propag.*, Vol. 35, No. 11, 1248–1257, 1987.
14. Mäkinen, R. M., J. S. Juntunen, and M. A. Kivikoski, "An improved thin-wire model for FDTD," *IEEE Trans. Microw. Theory Techn.*, Vol. 50, No. 5, 1245–1255, 2002.
15. Noda, T. and S. Yokoyama, "Thin wire representation in finite difference time domain surge simulation," *IEEE Trans. Power Delivery*, Vol. 17, No. 3, 840–847, 2002.
16. Railton, C. J., D. L. Paul, I. J. Craddock, and G. S. Hilton, "The treatment of geometrically small structures in FDTD by the modification of assigned material parameters," *IEEE Trans. Antennas Propag.*, Vol. 53, No. 12, 4129–4136, 2005.
17. Taniguchi, Y., Y. Baba, N. Nagaoka, and A. Ametani, "An improved thin wire representation for FDTD computations," *IEEE Trans. Antennas Propag.*, Vol. 56, No. 10, 3248–3252, 2008.
18. Taflove, A. and S. C. Hagness, *Computational Electrodynamics: The Finite-Difference Time-Domain Method*, 3rd Edition, Artech House, 2005.
19. Balanis, C. A., *Advanced Engineering Electromagnetics*, Wiley, New York, 1989.